Evaluation of Aerodynamic Noise Generation by a Generic Side Mirror

Yiping Wang, Zhengqi Gu, Weiping Li and Xiaohui Lin

Abstract—The aerodynamic noise radiation from a side view mirror (SVM) in the high-speed airflow is calculated by the combination of unsteady incompressible fluid flow analysis and acoustic analysis. The transient flow past the generic SVM is simulated with variable turbulence model, namely DES Detached Eddy Simulation and LES (Large Eddy Simulation). Detailed velocity vectors and contour plots of the time-varying velocity and pressure fields are presented along cut planes in the flow-field. Mean and transient pressure are also monitored at several points in the flow field and compared to corresponding experimentally data published in literature. The acoustic predictions made using the Ffowcs-Williams-Hawkins acoustic analogy (FW-H) and the boundary element (BEM).

Keywords—Aerodynamic noise, BEM, DES, FW-H acoustic analogy, LES

I. INTRODUCTION

OVER the past few years, with the rapid development of computation power and CFD technique, the field of Computational Aero Acoustics (CAA) became more and more relevant for the industrial applications, and this method had been applied in the area of the aero space industry commonly. Concerning the comfort of driver, more and more attention is paid to noise in the car development process. Flow induced noise, generated by additional device at the vehicle body, i.e. side mirrors, antennas or spoilers are especially important [1-6].

According to the view of fluid dynamic, the side view mirror (SVM) is a bluff body exposed to a high speed flow. The flow structure in the wake of the SVM is highly transient and will generate strong pressure fluctuation on the door panels and windows. This unsteady pressure fluctuation ultimately propagates into the carriage and exterior as noise.

Yiping Wang is with the State Key Laboratory of Advanced Design and Manufacture for vehicle Body National Institute of Standards and Technology, Hunan University, Changsha, CO 410082 China (corresponding author to provide phone: 86-0731-88823055; fax:86-0731-88823055; e-mail: yipingwang84524@ yahoo.com.cn).

Zhengqi Gu, is with the State Key Laboratory of Advanced Design and Manufacture for vehicle Body National Institute of Standards and Technology, Hunan University, Changsha, CO 410082 China (e-mail: guzhengqi63@sina.com).

Weiping Li, is with the State Key Laboratory of Advanced Design and Manufacture for vehicle Body National Institute of Standards and Technology, Hunan University, Changsha, CO 410082 China.

Xiaohui Lin, is with the State Key Laboratory of Advanced Design and Manufacture for vehicle Body National Institute of Standards and Technology, Hunan University, Changsha, CO 410082 China.

In this paper, the noise radiation from a SVM, which is positioned on a plate(Fig.1),is calculated by the combination of incompressible fluid flow analysis using the commercial CFD code FLUENT with LES and DES turbulence model and acoustic analysis using the Ffowcs-Williams-Hawkins acoustic analogy and boundary element method (BEM).

There are few applications of the acoustic analysis to the aerodynamic noise radiation problem from a high-speed automobile. The objectives of this calculation are to verify the accuracy of variable turbulence models and variable acoustic prediction in the analysis, to understand the mechanism of the aerodynamic noise radiation and to estimate the noise radiated from a SVM.

II. ANALYSIS PROCEDURE

Although it is appealing to calculate the aerodynamic noise radiation through a direct solution of a compressible Navier-Stokes equation, it is virtually impossible using exiting computers. The main reasons are as follows:

1) Sound pressure at an observation point, which is sometimes quite far from a noise source, is much smaller than the pressure fluctuation close to the noise source. Therefore, it is very difficult to accurately analyze both the noise source and its propagation simultaneously.

2) When it is required to calculate the sound pressure level (SPL) at a point far from a noise source, the analysis region must be large and the number of degrees of freedom of the problem becomes very large.

Then, the problem should be divided into two sequential parts. Firstly, the unsteady flow field around the mirror and the plate is analyzed to get the noise source, and secondly, the acoustic propagation from the surface to far field is analyzed. Tow assumptions are made here as following:

1) The flow field is not influenced by the acoustic field because the power of the acoustic field is much smaller than that of the flow field.

2) The fluid flow can be treated as incompressible because the Mach number is small enough in this calculation.

The effect of the motion of the medium on the noise propagation can be neglected because the Mach number is small enough in this calculation.

III. THE GENERIC SIDE MIRROR

To understand the nature of a phenomenon, it is well known that one has to start with a simple model, in order to reduce the complexity of the system. This was definitely one reason for Hold et al. [1] and Siegert et al. [2], have reported detailed

experimental measurements of the flow and acoustic fields around a generic SVM shape, from the point of view of creating a benchmark data set that can be used to test CFD and aero-acoustic codes. They also report results of analogous CFD and aeroacoustic simulations. By all means, they enriched the field of CAA by a simple test case, augmented with ample measurements, which declares the popularity of this model.

A. Geometry and test case

The geometry used in the present work consisted of a simplified SVM mounted on a flat plate. The mirror was composed of a half-cylinder 0.2m in diameter as well as in length topped by a quarter of a sphere of the same diameter. It was mounted on a flat plate 1.6m wide, 2.4 m long; the mirror was mounted 0.9m downstream of the elliptically shaped leading edge of the flat plate as illustrated in Fig. 1. This computational model accurately replicates the geometry considered by Hold et al. [1] and Siegert et al. [2] in their experimental study, and in this paper the experiment data will be referenced to validate the feasibility of the simulation.
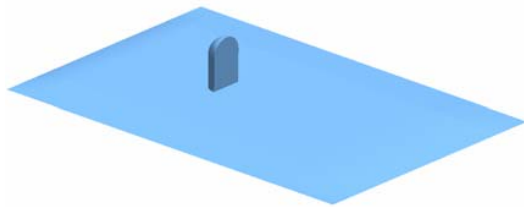

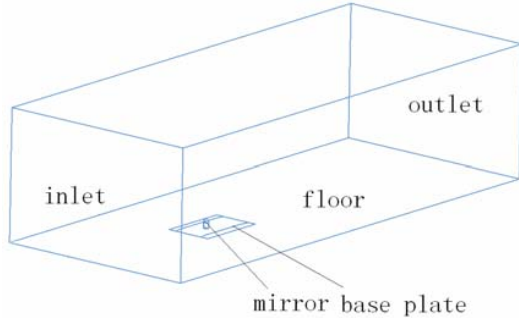
Fig. 1 The generic side view mirror and the base plate

Fig. 2 Computational domain around the side view mirror

B. Mesh and boundary conditions

A cuboid computational domain was used to obtain the CFD solution in this approach. It is illustrated in Fig.2.The mesh was created in the commercial software ICEM-HEXA. An unstructured hexahedral mesh was created in the entire domain. The mesh edge length was kept at 0.003m on the mirror and on the base plate in the vicinity of the mirror. Two views of the mesh are depicted in Fig. 3. The fine mesh was extended in the wake of the mirror till a distance of 1m from the mirror's rear face as seen in Fig. 3(a) and 3(b). The mesh was progressively coarsened from the vicinity of the mirror to the domain boundary where the mesh edge length was kept at 0.1m. The boundary conditions for the different surfaces bounding the computational domain are listed in Table 1.
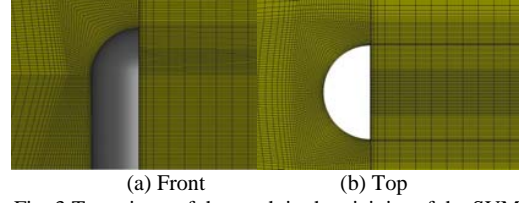

(a) Front   (b) Top

Fig. 3 Two views of the mesh in the vicinity of the SVM

TABLE I BOUNDARY CONDITIONS

Boundary	Boundary Condition	Value
Inlet	Constant Velocity	38.9m/s
Outlet	Constant Pressure	0Pa(gage)
Floor	Symmetry	—
Plate	No slip wall	—
Mirror	No slip wall	—
Other wall	Free slip wall	—

C. Turbulence models and Solver settings

Being interested in computing the aero acoustic noise sources, an appropriate resolution of the vortex structure of the flow field must be guaranteed. Thus, this means that one has to think about a suitable turbulence model to resolve the small scale oscillations, stemming from the fluctuating behavior of the in-stationary flow. This is always a balance between resolution, chosen turbulence model and computation time.

However, working experience as well as literature studies show, that a simple URANS (Unsteady Reynolds –Averaged - Navier -Stokes) solution with a standard turbulence models like $k-\varepsilon$, $k-\omega$ and SST are not resolve the time dependent nature of the flow properly for all relevant scales, and not really suitable for aero acoustic computation. It is important, to choose more sophisticated turbulence models. Thus, an appropriate choice would be a LES (Large Eddy Simulation) to resolve at least the big vortex structures and model only the scales beneath the grid size and DES(Detached Eddy Simulation) to resolve 'detached' eddies while wall-attached eddies are modeled.

In the simulation the LES approach uses the Smagorinsky-Lilly sub-grid scale model for eddy viscosity which is expressed as [7],

$$\mu_t = \rho[0.42d, C_s V^{1/3}]^2 \left| C_s \sqrt{2\overline{S_{ij}}.\overline{S_{ij}}} \right|$$

where, ρ is the density, d is the distance from the closest wall, V is the volume of the computational cell, $\overline{S_{ij}}$ is the rate of strain tensor, and C_s is a constant with a value 0.1. The LES model automatically uses the following laminar stress-strain relationship to compute wall shear stress if the mesh resolution is found to be fine enough to resolve the laminar sub-layer[8],

$$\frac{\overline{u}}{u_\tau} = \frac{\rho u_\tau y}{u}$$

Where, $\overline{u}$ is the mean velocity, u_τ is the friction velocity, y is distance from the wall, and u is dynamic viscosity. If the mesh is found to be too coarse to resolve the laminar sub-layer, the law-of-the-wall [9] is automatically applied.

The DES models, often referred to as the hybrid LES/RANS models combine RANS modeling with LES for applications such as high-Re external aerodynamics simulations. In this approach, the unsteady RANS models are employed in the near-wall regions, while the filtered versions of the same models are used in the regions away from the near-wall. The LES region is normally associated with the core turbulent region where large turbulence scales play a dominant role. In this region, the DES models recover the respective subgrid models. In the near-wall region, the respective RANS models are recovered. The computational costs, when using the DES models is less than LES computational costs, but greater than RANS.

In this paper, the DES model is based on the realizable $k - \varepsilon$ model, which is similar to the Realizable $k - \varepsilon$ model discussed in the literature [10], with the exception of the dissipation term in the k equation. In the DES model, the Realizable $k - \varepsilon$ RANS dissipation term is modified such that:

$$Y_k = \frac{\rho k^{\frac{3}{2}}}{l_{des}}$$

Where $l_{des} = \min(l_{rke}, l_{les})$

$$l_{rke} = \frac{k^{\frac{3}{2}}}{\varepsilon}$$

$$l_{les} = C_{des}\Delta$$

Where C_{des} is a calibration constant used in the DES model and has a value of 0.61 and Δ is the maximum local grid spacing ($\Delta x, \Delta y, \Delta z$).

In the paper the fluid flow analysis is based on the commercial CFD code Fluent, which is based on the finite volume method and provides a choice of solvers and settings. The settings chosen for this study are listed in Table 2.

TABLE II SOLVER SETTINGS USED IN THE SIMULATION

Function	setting
solver	Segregated implicit
	Double precision
Time-stepping	2nd order implicit
Pressure discretization	2nd order
Momentum discretization	2nd order upwind
Pressure-velocity coupling	SIMPLE
fluid	Air

D. Solution Procedure

A steady state solution was first obtained using RNG $k - \varepsilon$ turbulence model and 2nd discretization schemes. The steady state data was then used to initialize the transient LES and DES run. The transient simulation was started with an initial time-step of 0.003 second. Static pressure was monitored at a point behind the wake of the mirror. The amplitude and frequency of pressure fluctuations at this point were observed to discern when the solution reached dynamic stability. After achieving dynamic stability, the time-step was gradually reduced to 0.0001s and recording of acoustic source data was

started. The time-step size was maintained at this value for the rest of the simulation. Twenty solver iterations were conducted within each time step to ensure that the continuity and momentum equations were converged till the residuals dropped more than 3 orders of magnitude, at each time step.

E. Fluid Flow Analysis Results

Fig.4 shows the locations of pressure sensors.
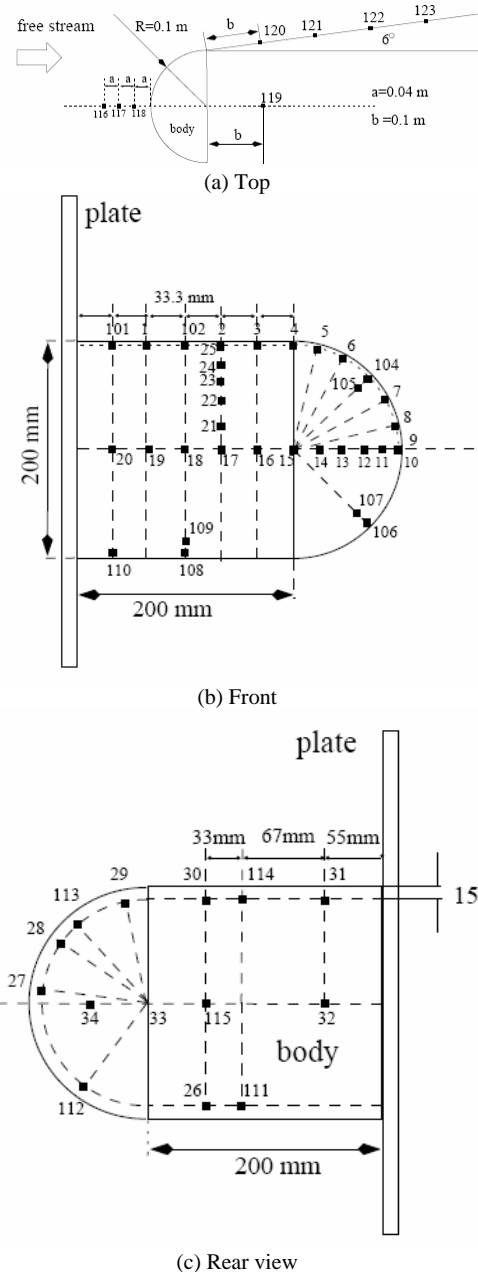

(a) Top

(b) Front

(c) Rear view
Fig. 4 Pressure sensor locations (Hold [1] et al.)

Fig.5 illustrates the performance of the CFD procedure by means of the predicted time-mean pressure coefficient. The sensor positions are taken from Figures 4b and 4c. The agreement between the predicted and measured data is reasonable, thus both the turbulence models can be availability to predict the transient flow field.
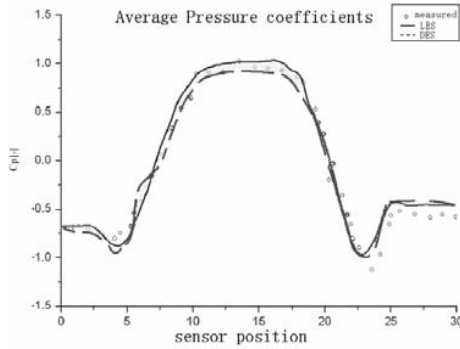
Fig. 5 Comparison of predicted and measured time-mean pressure coefficient

Instantaneous velocity contours and streamlines along the symmetry plane of the domain (z=0) are shown in Fig. 6. The mirror is seen to cause a large, complex wake with eddies spanning a range of scales and the separation region extends over a distance roughly double the mirror height (0.3 m). With two different turbulences, the wake behind the SVM is pretty much the same thing on the whole, but there are also some differences, so PIV experiment is necessary to validate the wake behind the SVM.
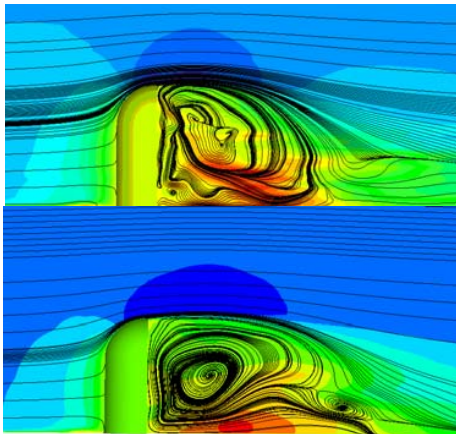

Fig. 6 Instantaneous velocity contours and streamline along the symmetry returned by LES (up) and DES (down)

Fig.7 illustrates the predicted p'_{rms} values obtained from the LES and DES simulations. The figure shows the shear layers over the cylindrical part of the mirror are the dominating cause to the sound generation. The comparison reveals that in the DES simulation the club-shaped structures are less pronounced and the high intensity region is smaller than the LES results.
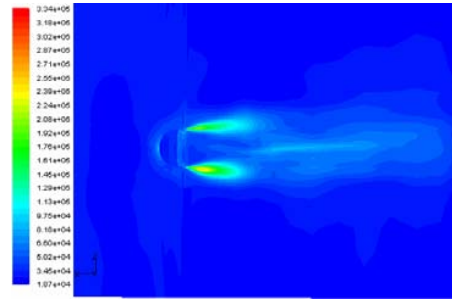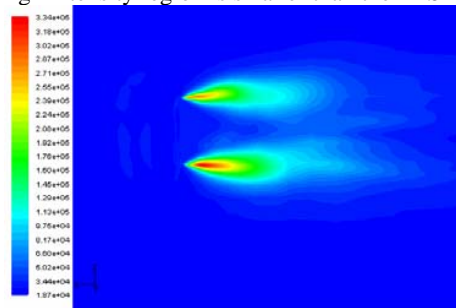

Fig. 7 Surface values of p'_{rms} returned by LES approach (up) and DES approach (down).

For automotive applications the wall pressure levels is by far the most important result. The wall pressure represents the physical excitation of the exterior structure and from the driver or passengers point of view the radiated sound at a location outside the compartment is of less interest. The fluctuating pressure level presented in this paper is computed in the following way:

$$PFL = 10\log10\frac{\hat{p}}{p_{ref}^2}$$

Where $p_{ref} = 2 \times 10^{-5}$ (Pa) is the reference pressure and $\hat{p}$ is power spectral density of the fluctuating pressure. The presentation of hydrodynamic pressure fluctuations in terms of SPL can be somewhat misleading as sound pressure levels only account for emissions in the far field. For this reason, the power density spectrum of fluctuating hydrodynamic pressure levels is denoted as Pressure Fluctuating Levels (PFL) instead. Figures 8 to 12 present the computed results as well as the Hold et al. and Siegert et al. measurements for comparison.
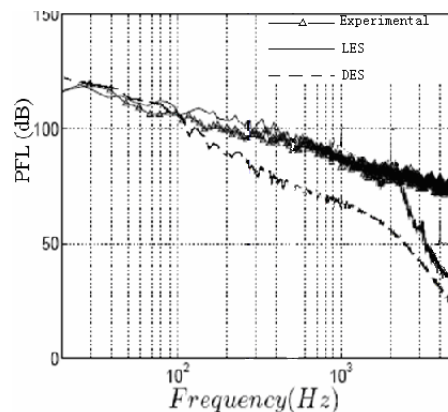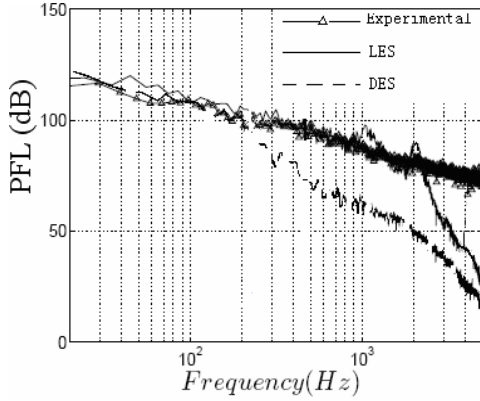

Fig. 8 PFL at surface sensor 111
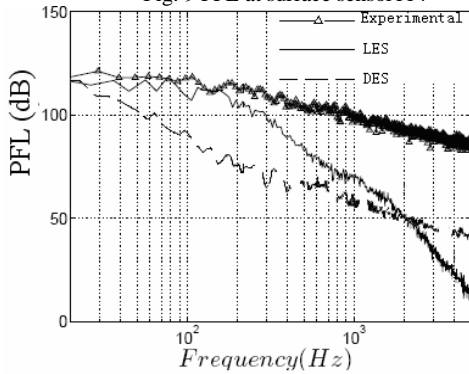
Fig. 9 PFL at surface sensor114
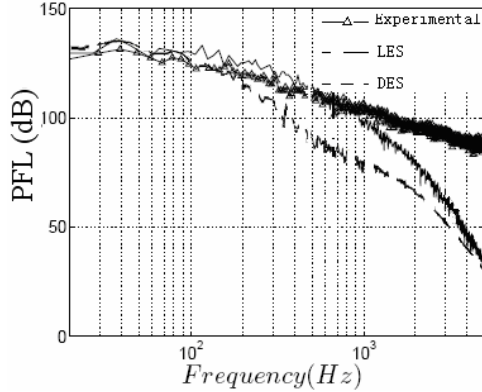

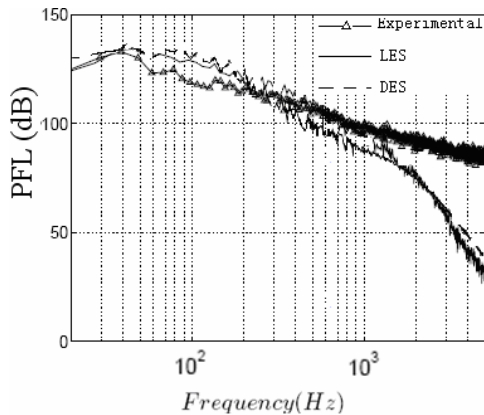Fig. 10 PFL at surface sensor 116

Fig. 11 PFL at surface sensor 121

Fig. 12 PFL at surface sensor 123

The results collected from the two sensors located on the rear side of the mirror are presented in Figs8 and 9. From these figures it is clear that DES model predicts quite accurate below 100Hz and underpredict the source levels over100Hz while the LES models predicts the levels fairly accurate all the way to the resolved cut-off frequency. Above the resolved cut-off frequency several peaks in the LES signals are seen which may be due to aliasing effects. For the wall pressure levels this is of no concern since it occurs outside the valid frequency range. For sensor 116 presented in Fig.10 the discrepancy between the two simulations is even more pronounced. The location of this sensor is close to the horse-shoe vortex upstream the mirror and a misrepresentation in size and location can cause the discrepancy in results. The misrepresentation at this location is however expected due to the low resolution over the plate, and for the DES case maybe the RANS treatment of the boundary layers preventing fluctuations to occur too. For the sensors located in the high level region behind the mirror 121 and 123 the DES case show similar results as the LES case in the low frequency region although drops rapidly when reaching the resolved cut-off frequency. If this is caused by the discretization scheme or due to the turbulence model or a combination of both is unclear and should be investigated further.

A general trend for the wall pressures results is that the levels are underpredicted by the DES model but overpredicted with the LES approach. An overprediction would intuitively be expected due to the incompressible assumption, but in the same time LES will expend much more computer source than DES, so the selection of LES or DES must be caution in practical engineering applications.

IV. ACOUSTIC ANALYSIS

The area of aero acoustics is deeply combined with the name of Lighthill, which he pioneered with his first paper [11]. There, starting from the Navier-Stokes Equation he rewrites them and derives one scalar equation for the propagation of sound.

To repeat this proceeding shortly, Lighthill used the continuity equation

$$\frac{\partial \rho}{\partial t} + \frac{\partial \rho u_i}{\partial x_i} = 0 \,, \tag{1}$$

and the momentum equation

$$\frac{\partial \rho u_i}{\partial t} + \frac{\partial \rho u_i u_j}{\partial x_j} = -\frac{\partial p}{\partial x_i} + \frac{\partial \tau_{ij}}{\partial x_j} \,, \tag{2}$$

where

$$\tau_{ij} = (\left(\frac{\partial u_i}{\partial x_j} + \frac{\partial u_j}{\partial x_i} - \frac{2}{3}\frac{\partial u_k}{\partial x_k}\delta_{ij} \right)$$

is the viscous stress tensor for a Newtonian fluid.

Differentiating (1) with respect to time, in order to derive a wave equation like operator, and subtracting the divergence of (2) leads to a scalar equation of the form

$$\frac{\partial^2 \rho}{\partial t^2} + \frac{\partial^2 \rho u_i u_j}{\partial x_i \partial x_j} = -\frac{\partial^2 p}{\partial x_i^2} + \frac{\partial^2 \tau_{ij}}{\partial x_i \partial x_j}.$$

Moving the convective term to the right hand side and adding an additional term $-c^2 \partial^2 \rho / \partial x_i^2$ on both sides, one gets a wave equation for the density, i.e.

$$\frac{\partial^2 \rho}{\partial t^2} - c^2 \frac{\partial^2 \rho}{\partial x_i^2} = \frac{\partial^2 \tau_{ij}}{\partial x_i \partial x_j} \quad , \tag{3}$$

Here, $T_{ij} = \upsilon u_i u_j - \tau_{ij} + (p - c^2 \rho)\delta_{ij}$ is called the Lighthill tensor, and c is the speed of sound. The Equation (3) is well known as Lighthill's Equation.

In this paper, the Ffowcs-Williams-Hawkins acoustic analogy and the boundary element method (BEM) were adopted to predict the far field sound pressure.

A The Ffowcs-Williams-Hawkins Acoustic Analogy

An extension of Lighthill's Equation, to the presence of solid surfaces was first done by Curle[12]and later extended by Ffwocs Williams and Hawkings[13] to surfaces in arbitrary motion. There equation reads as

$$\frac{\partial^2 \rho}{\partial t^2} - c^2 \frac{\partial^2 \rho}{\partial x_i^2} =$$

$$\frac{\partial}{\partial t}\{\rho_0 v_n \delta(f)\} - \frac{\partial}{\partial x_i}\{p_{ij}\delta(f)\} + \frac{\partial^2 T_{ij}}{\partial x_i x_j} \tag{4}$$

where the source terms on the right-hand side describe monopole, dipole and quadrapole terms, respectively. For a stationary surface, one can neglect the monopole terms.

Doing this, the dipole and quadrapole terms were compared. The intensity for dipole term is proportional to the flow velocity i.e.

$$I_D \approx \rho u^6 c^{-3} l^2 , \tag{5}$$

and for the quadrapole term

$$I_Q \approx \rho u^8 c^{-5} l^2 , \tag{6}$$

Thus, comparing (5) and (6), getting for the ratio of both

$$\frac{I_Q}{I_D} \propto \left(\frac{u}{c}\right)^2$$

Considering a Mach number $Ma = u/c$ around 0.16, i.e. u = 38.9 m/s, the intensity of the quadrapole term was approximately one percent of the dipole terms, i.e.

$$I_Q \propto 0.0131 I_D$$

Thus, the dipole source was the main noise sources for noise generation, rather than the quadrapole sources in the turbulent flow field. This means, that the key of research is the pressure fluctuations on the solid surface, e.g. the side window as the dominant cause for the noise generation.

B The Boundary Element Method (BEM)

It is well known that the FW-H acoustic analogy can work when the receiver is located in the computer domain interior. However, if the receiver is far from the sound source and the computer domain is not so large that the receiver is in its interior, so the boundary element method [14] is adopted to solve this problem(of course in this paper in order to compare to the experimental data the receiver is in the domain interior).

The noise propagation problem with time-harmonic load is described by the Helmholtz equation with boundary conditions. $\Delta p + k^2 p = 0$, with $p = \bar{p}$ or $\nabla_n p = \overline{\nabla_n p}$ on boundary surface, Where p is the acoustic pressure, k is the wave number defined as $2\pi f/c$ (f is frequency, c is sound velocity), ∇_n is the normal derivative operator and means given boundary condition value.

This problem can be rewritten in the boundary integral equation, which is numerically solved using BEM. SPL at a given observation point can be calculated from the obtained p and $\nabla_n p$ values on boundary surface using the Green function. This calculation is carried out using the commercial BEM code SYSNOISE acoustic code.

The boundary condition of prescribed pressure (condition) is imposed on the mirror and plate surface, by applying a discrete Fourier transformation to the pressure fluctuation data of fluid flow analysis.

C Acoustics Analysis Result

Fig.13 shows the location of acoustic receivers, and the coordinates of acoustics receiver locations are listed in table 3.
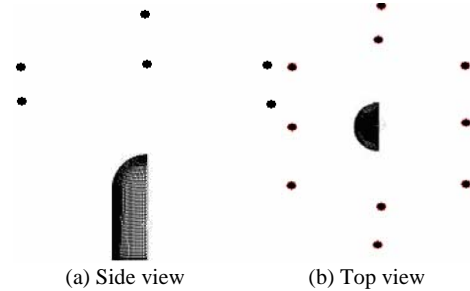

(a) Side view   (b) Top view

Fig.13 Microphone positions employed for the assessment of the acoustic results (Siegertet al. [2])

TABLE III COORDINATES OF ACOUSTICS RECEIVER LOCATIONS

Point	x(m)	y(m)	z(m)
101	-0.35	0.35	-0.25
102	-0.35	0.435	0
103	-0.35	0.35	0.25
104	0	0	-0.5
105	0	0.453	-0.35
106	0	0.6	0
107	0	0.453	0.35
108	0	0	0.5
109	0.35	0.453	-0.35
110	0.35	0.6	0
111	0.35	0.453	0.35

Note: The origin is located on the top surface of the base plate at the mid point of the flat surface of the mirror. The negative x axis is in the flow direction, the positive y axis points from the origin to the apex of the mirror and the z axis is along the spanwise direction.

Fig.14 compares the measured sound pressure levels at various microphone positions with results provided by the FW-H procedure and the BEM

(a) 101

(b) 102

(c) 104
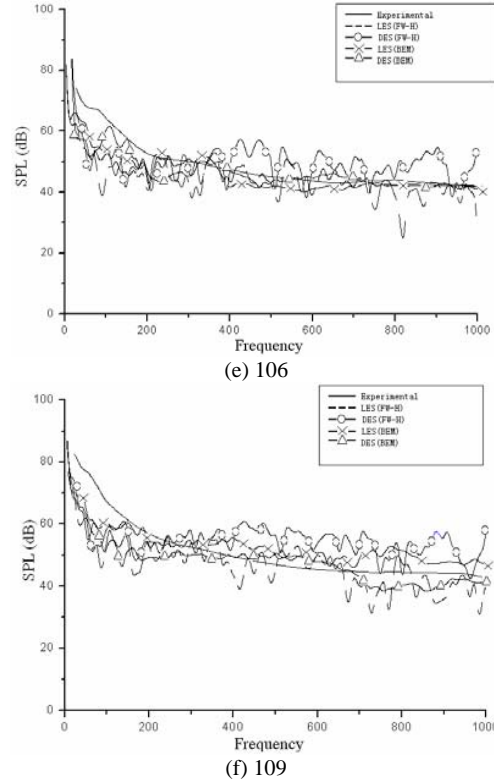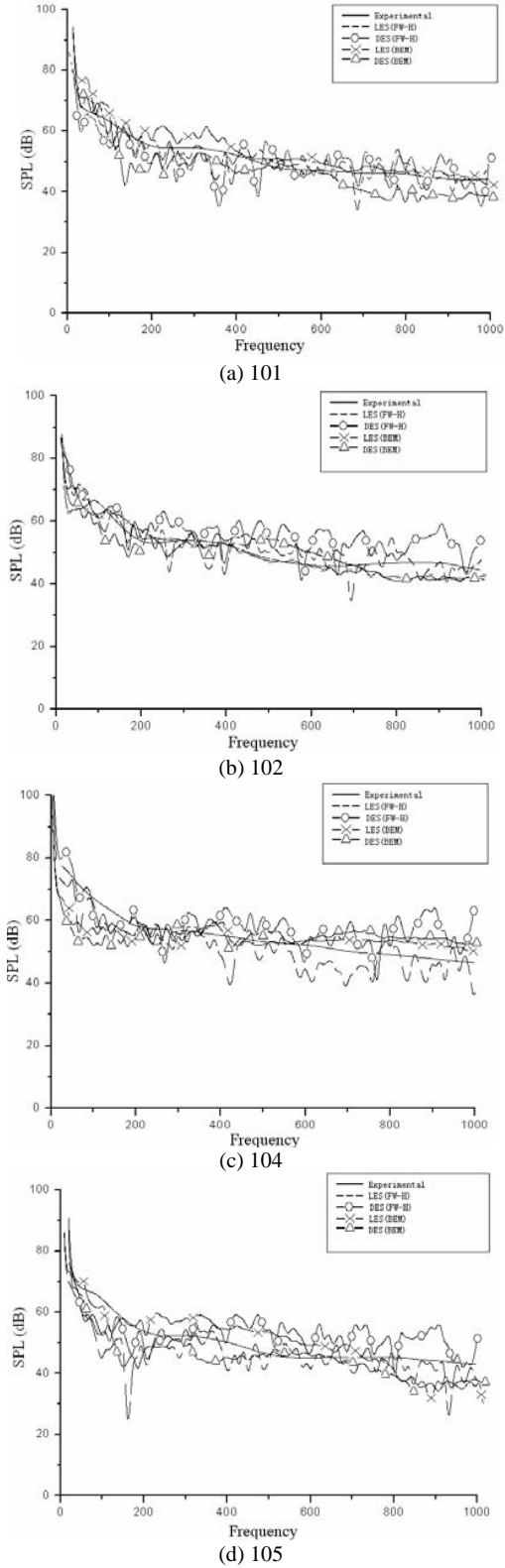

(d) 105

(e) 106

(f) 109

Fig.14 Sound pressure levels at microphones returned by the FW-H and BEM

Fig.15 shows the dipole source on the mirror and plate surface, comparing to the fig.7 it reveals that the p'_{rms} is large where the intensity of the sound source is strong.

Fig.15 The dipole source on the mirror and plate surface returned by LES (up) and DES (down) (f=30Hz)

Fig.16 shows the sound field around the mirror, and it posts that the main noise source locates the rear of the mirror.
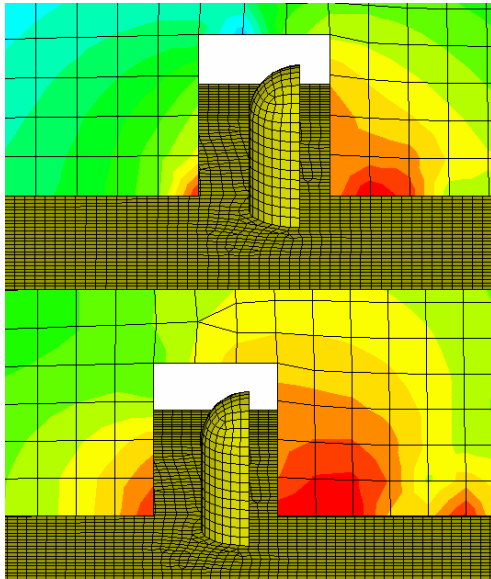
Fig. 16 the sound filed around the mirror returned by LES (up) and
DES (down) (f=30Hz)

V. CONCLUSIONS

In this paper the first attempt is made to predict both the flow
field and emitted sound pasting a generic side mirror mounted
on a at plate. The Reynolds number is 5.2×10^5 basing on mirror
diameter; the corresponding Mach number for this flow field is
Ma = 0.11. Owing to the low Mach number, the flow field is
solved on the basis of an assumption of incompressibility.

The present simulation attempts to capture this flow field by
two different turbulence models with the same mesh. The first
one is by using the LES model and in the second approach the
DES model is used. The sound propagation is calculated also by
two different approaches. One is the Ffowkes-Williams and
Hawkings analogy, the other is the boundary element (BEM).
The overall conclusions drawn from the present simulation are
as follows:

1) In the prediction of the wall pressure fluctuations the trend
   is pretty much the same thing when these two different
   turbulence models are used, and the LES is more accurate
   than the DES. However the LES will expend much more
   computer source than DES.

2) The mechanism of the aerodynamic noise radiation is
   revealed. The noise is mainly radiated from the place where
   the strong vortices that are shed from the mirror.

3) Using the FW-H and BEM to predict the sound propagation
   is considered to be feasible, and the BEM can be used to
   predict the noise characteristic when the receiver is located
   outside the computer domain.

REFERENCES

[1] Hold, R., Brenneis, A., and Eberle, A., "Numerical Simulation of
     Aeroacoustic Sound Generated by Generic Bodies Placed on a Plate: Part
     I - Prediction of Aeroacoustic Sources," 5th AIAA/CEAS Aeroacoustics
     Conference. Seattle, Washington, 10-12 May 1999, pp. AIAA-99-1896.

[2] Siegert, R., Schwartz, V., and Reichenberger, J., "Numerical Simulation
     of Aeroacoustic Sound Generated by Generic Bodies Placed on a Plate:
     Part II - Prediction of Radiated Sound Pressure," 5th AIAA/CEAS
     Aeroacoustics Conference. Seattle, Washington, 10-12 May 1999, pp.
     AIAA-99-1895.

[3] Bipin Lokhande, Sandeep Sovani and Jieyong Xu.Computational
     Aeroacoustic Analysis of a Generic Side View Mirror SAE paper
     2003-01-1698 (2003).

[4] Jonas Ask and Lars Davidson .The Sub-critical Flow past a Generic Side
     Mirror and its Impact on Sound Generation and Propagation 12th
     AIAA/CEAS Aeroacoustics Conference. Cambridge, Massachusetts,
     8-10 May 2006 AIAA 2006-2558.

[5] Th. Rung, D. Eschricht, J. Yan and F. Thiele. Sound Radiation of the
     Vortex Flow Past a Generic Side Mirror 8th AIAA/CEAS Aeroacoustics
     Conference & Exhibit, Breckenridge, Colorado, 17-19 June 2002 AIAA
     2002-2549.

[6] Thorsten Grahs and Carsten Othmer. Evaluation of aerodynamic noise
     generation: parameter study of a generic side mirror evaluating the
     aeroacoustic source strength. European Conference on Computational
     Fluid Dynamics (2006).

[7] Sagaut, P.: Large-Eddy Simulation for Incompressible Flows, 3rd edn.
     Scientific Computation. Springer, Berlin Heidelberg New York (2005).

[8] E. de Villiers. The potential of large eddy simulation for the modeling of
     wall bounded flows. PhD thesis, Imperial College London (2005).

[9] Tennekes, H. and Lumley, J.L., A First Course in Turbulence, MIT Press,
     Cambridge, MA (1972).

[10] Fluent 6.3 User's Guide, Fluent Inc.

[11] M. J. Lighthill. On sound generated aerodynamically, I General theory.
     Proc. Roy. Soc., A 211, 564–587, (1952).

[12] N. Curle. The influence of solid boundaries upon aerodynamic sound.
     Proc. Roy. Soc., A 231, 505–514, (1955)..

[13] J. E. Ffowcs Williams and D. L. Hawkins. Sound generation by
     turbulence and surfaces in arbitrary motion. Sound. Philos. Trans. Roy.
     Soc., A 264, No. 1151, 321–342, (1969).

[14] Numerical Acoustics Theoretical Manual. LMS International.